

Langevin / Monte Carlo Treatment of Coulomb Collisions in PIC Simulations*

Martin Lampe, Wallace M. Manheimer, Glenn Joyce, and Steven P. Slinker
Plasma Physics Division, Naval Research Laboratory
Washington, DC 20375-5346

* Supported by Office of Naval Research

1. Introduction

Efficient techniques are available for representing electron-neutral and ion-neutral collisions within particle-in-cell / Monte Carlo (PIC / MC) codes [1], but Coulomb collisions are usually omitted because it is difficult to treat them efficiently. This can lead to serious errors, particularly because Coulomb collisions are essential in populating the high-energy tail, and thus driving the distribution toward Maxwellian.

It is extremely inefficient to represent Coulomb collisions as two-body interactions mediated by the shielded Coulomb potential, since time steps smaller than the plasma period are required, and even on this very short time scale any given electron will be scattering off many other particles simultaneously. A better approach is to use the Fokker-Planck equation, which in effect sums up the frictional and diffusive effects of many small-angle Coulomb scatterings, and thus permits the use of much longer time steps. Takizuka and Abe [2] developed a binary collision model, based on the direct-simulation Monte Carlo technique of Bird [3], but with the collision cross-section representing the Fokker-Planck process. This approach has the correct properties and conserves energy and momentum exactly, but the accounting associated with pairwise collisions is complex and rather slow. An efficient alternative approach, developed recently by Jones et al [4], is to calculate the Fokker-Planck coefficients on the grid, transform the Fokker-Planck equation into an equivalent Langevin equation, and use a Monte Carlo method to scatter individual particles according to the Langevin equation. However, in [4] the diffusion was assumed to be isotropic and independent of the particle velocity v , the friction coefficient was assumed to be proportional to v , and both the friction and diffusion coefficients were assigned the Spitzer values, which are mean values based on an isotropic Maxwellian distribution of scatterers. These assumptions limit the usefulness of the formulation, particularly because the correct friction and diffusion coefficients fall off rapidly for superthermal particles. In situations where Coulomb collisions are in competition with other processes which drive the electron distribution *away* from Maxwellian (e.g., inelastic electron-neutral collisions which extract energy from the high-energy electrons), inattention to this velocity dependence can strongly distort the high-energy part of the electron distribution.

In this paper, and in more detail in Ref. 5, we extend the Langevin / Monte Carlo approach of Jones et al by properly including the velocity dependence of the friction and random walk, and properly representing the anisotropic nature of the random walk. We do need to retain one key approximation to reduce the scattering process to a numerically tractable form: the scatterer velocities are treated as if they are distributed isotropically in their center-of-mass frame. We have shown [5] that the method is highly accurate for anisotropy aspect ratios up to about two, and that the isotropy requirement applies only to the thermal part of the scatterer distribution. In many applications, this limitation is quite acceptable, since isotropization typically proceeds much more rapidly than other processes of interest, such as Maxwellianization of the high-energy tail. In those cases where the isotropic-scatterer assumption is a serious limitation, better results can still be obtained efficiently by representing the scatterer distribution as a superposition of several isotropic distributions displaced from each other in velocity space.

2. Formalism

The standard form [6] of the Fokker-Planck equation for shielded Coulomb scattering of particles of species 1 off particles of species 2 (species 1 and 2 may be the same) is

$$\left. \frac{\partial f_1}{\partial t} \right|_{12} = -\frac{\partial}{\partial \mathbf{v}} \cdot \mathbf{F}_d(\mathbf{v})f_1(\mathbf{v}) + \frac{1}{2} \frac{\partial^2}{\partial \mathbf{v} \partial \mathbf{v}} : \mathbf{D}(\mathbf{v})f_1(\mathbf{v}), \quad \text{where } \mathbf{F}_d(\mathbf{v}) = \frac{4\pi n e^4}{m_1^2} \lambda \frac{\partial H}{\partial \mathbf{v}}, \quad \mathbf{D}(\mathbf{v}) = \frac{4\pi n e^4}{m_1^2} \lambda \frac{\partial^2 G}{\partial \mathbf{v} \partial \mathbf{v}}, \quad (1)$$

$$\lambda = \ln\left(\frac{\csc\theta_m}{2}\right), \quad \theta_m = 2 \tan^{-1}\left(\frac{2e^2}{m_1 v_c^2 \lambda_D}\right), \quad \mathbf{H}(\mathbf{v}) = Z_1^2 Z_2^2 \frac{m_1 + m_2}{m_2} \int d^3 \tilde{\mathbf{v}} \frac{f_2(\tilde{\mathbf{v}})}{|\mathbf{v} - \tilde{\mathbf{v}}|}, \quad \mathbf{G}(\mathbf{v}) = Z_1^2 Z_2^2 \int d^3 \tilde{\mathbf{v}} f_2(\tilde{\mathbf{v}}) |\mathbf{v} - \tilde{\mathbf{v}}|. \quad (2)$$

In PIC codes, it is impractical (in terms of numbers of particles, computation time, and statistical fluctuations) to actually compute the coefficients $\mathbf{H}(\mathbf{v})$ and $\mathbf{G}(\mathbf{v})$ as multiple integrals, and then perform numerical differentiations. But if the scatterer distribution function $f_2(\tilde{\mathbf{v}})$ is a function of only the magnitude of the velocity, in the reference frame in which the scatterer fluid velocity \mathbf{u}_2 is zero, the Fokker-Planck equation can be reduced [5] to a much more tractable form, with

$$\mathbf{H}(\mathbf{v}) = \frac{8\pi}{v} \int_0^v d\tilde{v} \tilde{v}^2 f_2(\tilde{v}) + 8\pi \int_v^\infty d\tilde{v} \tilde{v} f_2(\tilde{v}), \quad \mathbf{G}(v) = \frac{4\pi}{3} \left[\int_0^v d\tilde{v} \tilde{v}^2 \frac{3v^2 + \tilde{v}^2}{v} f_2(\tilde{v}) + \int_v^\infty d\tilde{v} \tilde{v} (v^2 + 3\tilde{v}^2) f_2(\tilde{v}) \right]. \quad (3)$$

The velocity derivatives in $\mathbf{F}_d(\mathbf{v})$ and $\mathbf{D}(\mathbf{v})$, Eqs. (1), can then be calculated analytically from Eqs. (3), which greatly reduces noise in the simulation. We find $\mathbf{F}_d(\mathbf{v}) = F_d(v)(\mathbf{v}/v)$, with

$$\mathbf{F}_d(v) = \frac{4\pi n e^4}{m_1^2} \lambda \frac{d\mathbf{H}}{dv} = -\frac{16\pi^2 n e^4 Z_1^2 Z_2^2}{v^2} \frac{m_1 + m_2}{m_1^2 m_2} \lambda \int_0^v d\tilde{v} \tilde{v}^2 f_2(\tilde{v}). \quad (4)$$

Since \mathbf{G} is a scalar function of the scalar variable v , the tensor $\partial^2 \mathbf{G} / \partial v \partial \mathbf{v}$ is diagonal in a coordinate system with the 3-component parallel to \mathbf{v} . The only non-zero components of the tensor \mathbf{D} are D_{33} and $D_{11}=D_{22}$, with

$$D_{33}(v) = \frac{4\pi n e^4}{m_1^2} \lambda \frac{\partial^2 \mathbf{G}}{\partial v_3 \partial v_3} = \frac{4\pi n e^4}{m_1^2} \lambda \frac{d^2 \mathbf{G}}{dv^2} = \frac{32\pi^2 n e^4 Z_1^2 Z_2^2}{3m_1^2} \lambda \left[\frac{1}{v^3} \int_0^v d\tilde{v} \tilde{v}^4 f_2(\tilde{v}) + \int_v^\infty d\tilde{v} \tilde{v} f_2(\tilde{v}) \right], \quad (5a)$$

$$D_{11}(v) = \frac{4\pi n e^4}{m_1^2} \lambda \frac{\partial^2 \mathbf{G}}{\partial v_1 \partial v_1} = \frac{4\pi n e^4}{m_1^2} \lambda \frac{1}{v} \frac{d\mathbf{G}}{dv} = \frac{16\pi^2 n e^4 Z_1^2 Z_2^2}{3m_1^2} \lambda \left[\frac{1}{v^3} \int_0^v d\tilde{v} \tilde{v}^2 (3v^2 - \tilde{v}^2) f_2(\tilde{v}) + 2 \int_v^\infty d\tilde{v} \tilde{v} f_2(\tilde{v}) \right]. \quad (5b)$$

In a PIC code, these velocity-dependent integrals can be accumulated as grid quantities at the same time that the particle densities are laid down on the grid. One may wish to average these quantities over some appropriate spatial volume, to reduce the fluctuations resulting from the finite number of particles at any grid point.

If the distribution function $f_2(\tilde{\mathbf{v}})$ is not isotropic in any reference frame, we can still use (3-5) by defining and substituting an isotropized distribution $\bar{f}_2(|\tilde{\mathbf{v}} - \mathbf{u}_e|) \equiv (1/4\pi) \int_0^\pi d\theta \sin\theta \int_0^{2\pi} d\phi f_2(\mathbf{v})$.

The Fokker-Planck equation (1) is equivalent to the Langevin equation

$$\Delta \mathbf{v} = \mathbf{F}_d \Delta t + \mathbf{Q}, \quad (6)$$

where $\Delta \mathbf{v}$ is the change in a particle's velocity, due to e-e scattering, during an infinitesimal time step Δt , and \mathbf{Q} is a random velocity vector chosen from the distribution

$$\phi(\mathbf{Q}) = \frac{1}{(2\pi\Delta t)^{3/2} D_{11} D_{33}^{1/2}} \exp\left(-\frac{\mathbf{Q}_3^2}{2D_{33}\Delta t} - \frac{\mathbf{Q}_1^2 + \mathbf{Q}_2^2}{2D_{11}\Delta t}\right). \quad (7)$$

Using Eqs. (4) - (7) and taking averages over the stochastic variable \mathbf{Q} , one can show that energy and momentum are conserved, to first order in Δt , provided that the distribution function $f_2(\mathbf{v})$ is actually isotropic in its center-of-mass frame. However, small non-conservation errors can occur, due to: (i) second and higher order effects in Δt ; (ii) statistical fluctuations in the numerical average of \mathbf{Q} due to the finite number of particles; (iii) non-isotropy of $f(\mathbf{v}_2)$ in the frame chosen for use in Eqs. (3-5), or (worse yet) this frame not being the exact local center-of-mass frame; (iv) spatial smoothing of the coefficients. We shall discuss strategies for insuring exact conservation, and (a related point) for extending the time step Δt that may be used. The ultimate limitation on Δt is one of accuracy. Thus, Δt should be no more than a fraction of the e-e collisional relaxation time, or any shorter time scale imposed by other aspects of the simulation, e.g. the characteristic times for inelastic electron-neutral scattering, escape of electrons to the walls, etc.

For electrons scattering off ions, the rate of energy exchange is down by order m_e/m_i , which makes it negligible for many purposes. If we choose to neglect energy exchange and treat e-i scattering as simply pitch-angle scattering of the electrons off infinitely massive ions, then the formalism becomes particularly simple. It is then appropriate to approximate the ion velocities as zero, so that Eqs. (2) reduce to $H=Z_i^2/v$, $G=Z_i^2v$. According to Eqs. (5), the diffusion coefficients are $D_{33}(v) = 0$, $D_{11}(v) = D_{22}(v) = (4\pi n e^4 Z_i^2 / m^2 v) \lambda$. To insure that electron energy is conserved exactly in every collision, we can simply specify Δv_3 as the solution of $v^2 = (v+\Delta v_3)^2 + Q_1^2 + Q_2^2$, where Q_1 , Q_2 are the stochastic increments to the velocity components normal to \mathbf{v} , chosen from the distribution (7). If we neglect second order in Q_1/v and Q_2/v , this becomes simply $\Delta v_3 = (Q_1^2 + Q_2^2)/2v$.

3. Computational Examples

We present two simple computational examples as test cases. In each case, the Fokker-Planck coefficients (4,5) are computed over a spatially uniform region consisting of 35 cells and containing 15,000 macroparticles to represent the electrons. The electrons are scattered at intervals $\Delta t = 8 \times 10^{-9}$ sec.

A. Approach to Equilibrium

Here we consider the evolution of the electron distribution from an anisotropic and non-Maxwellian initial condition, with e-e scattering the only physical process represented in the simulation. The initial distribution is a flat-topped cylinder in velocity space,

$$f(v_z, v_\perp, t=0) = \frac{1}{2\pi v_{z0} v_{\perp 0}^2} \Theta(v_{z0} - |v_z|) \Theta(v_{\perp 0} - v_\perp), \quad (8)$$

where $v_\perp \equiv (v_x^2 + v_y^2)^{1/2}$, $\Theta(v)$ is the step function, $mv_{z0}^2/2 = 2$ eV and $mv_{\perp 0}^2/2 = 4$ eV. The plasma density is 10^{12} cm^{-3} . Since the Fokker-Planck coefficients decrease rapidly with v , the approach to equilibrium should proceed rapidly for electrons in the low-energy (thermal) range, and more slowly in the high-energy tail. Fig. 1 shows plots of the reduced electron distribution functions $f(v_\parallel) \equiv \int_0^\infty dv_\perp 2\pi v_\perp f(\mathbf{v})$ and $f(v_\perp) \equiv \int_{-\infty}^\infty dv_\parallel f(\mathbf{v})$ at four

different times. To exhibit Maxwellians as straight lines, the abscissa in these plots is chosen to be $\epsilon_z \equiv m_e v_z^2/2$ or $\epsilon_\perp \equiv m_e v_\perp^2/2$. Figure 1a shows the initial distributions. In Fig. 1b, at the early time [7] $t = 1 \times 10^{-8}$ sec, the distribution functions have become rounded but are still anisotropic and non-Maxwellian. In Fig. 1c, at $t = 7 \times 10^{-8}$ sec, the distribution is isotropic and close to Maxwellian in the thermal range, but is still anisotropic and non-Maxwellian in the high energy range. Finally, in Fig. 1d at time 2×10^{-7} sec, the distribution functions are isotropic and Maxwellian over their entire energy range.

B. Balance Between Heating, e-e Collisions, and Inelastic Collisions

In this example we model, in a very simplified way, the combined effect of several processes that occur in an electron cyclotron resonance (ECR) discharge: plasma heating, e-e collisions, and electron energy loss due to ionizing collisions. In the model, electrons with energy $\epsilon < 3$ eV are heated every time they pass by a "resonant zone" located at $z = 3$ cm, by giving each electron a velocity kick Δv chosen randomly from a Gaussian distribution with mean value $m(\Delta v)^2/2 = 1$ eV. We also include electron energy loss due to "ionizing collisions" with argon atoms: In the model, an electron loses exactly 15.76 eV of energy at each such collision. For these collisions, we use the ionization cross section for Ar, which increases from about 10^{-16} cm^2 just above $\epsilon_{iz} = 15.76$ eV, to a maximum of 3.9×10^{-16} cm^2 at 60 eV.

We run the simulation until the electron energy distribution function (EEDF) reaches equilibrium. Figure 2 shows the results for several cases with differing values of the plasma density n_e , but with neutral gas pressure equal to 5 mTorr in each case. The e-e collision rate is thus proportional to n_e , while the electron-neutral collision rate is the same for each case. In Fig. 2a, at plasma density 10^{10} cm^{-3} , electron-electron scattering is weak and ionization energy losses deplete the tail of the distribution function for energies above ϵ_{iz} . In Fig. 2b, at density 10^{11} cm^{-3} , e-e scattering is strong enough to drive the electron distribution to Maxwellian in the regime below ϵ_{iz} and to significantly replenish the distribution above the ionization threshold. In Fig. 2c, at density 10^{12}

cm^{-3} , e-e scattering is easily strong enough to redistribute energy from the heating region (mainly $\epsilon < 5$ eV) to the tail region, and the equilibrium distribution is very nearly Maxwellian over the entire energy range.

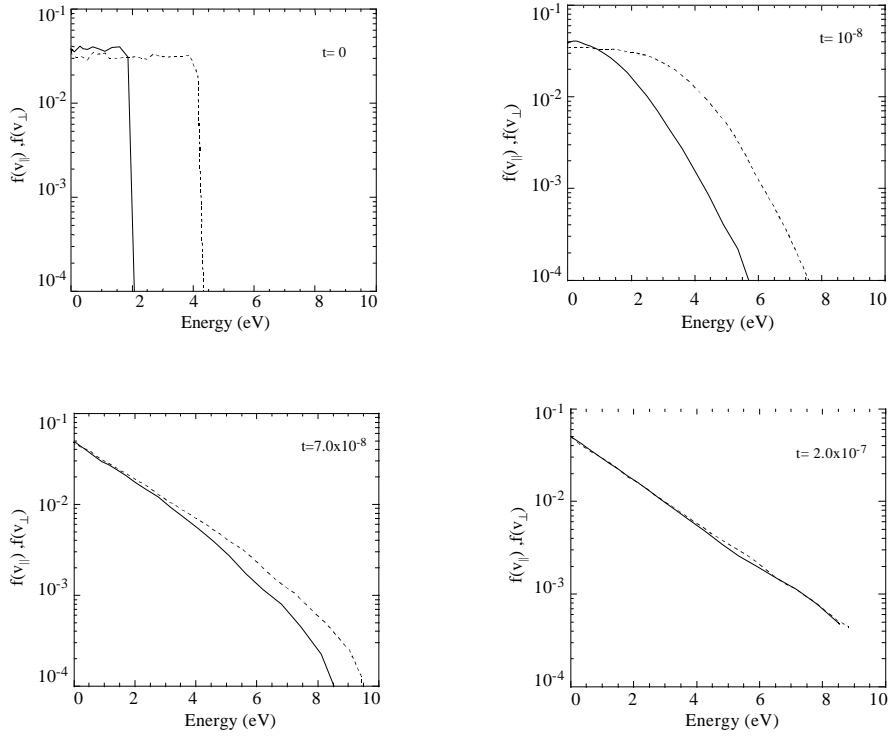


Fig. 1. Reduced electron distribution functions $f(v_{\parallel})$ (solid curve) and $f(v_{\perp})$ (dashed curve) at times (a) $t=0$, (b) 1×10^{-8} sec, (c) 7×10^{-8} sec, (d) 2×10^{-7} sec.

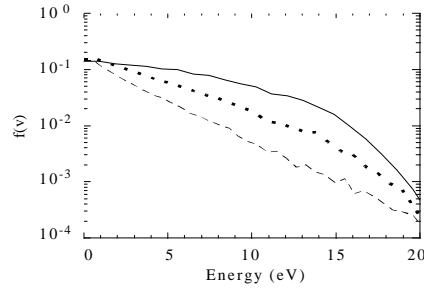


Fig. 2. Electron energy distribution functions for Ar at pressure 5 mTorr, after steady state has been reached. Solid curve: $n_e = 10^{10} \text{ cm}^{-3}$. Dotted curve: $n_e = 10^{11} \text{ cm}^{-3}$. Dashed curve: $n_e = 10^{12} \text{ cm}^{-3}$.

References

1. C. K. Birdsall, IEEE Trans. Plasma Sci. **19**, 65 (1991).
2. T. Takizuka and H. Abe, J. Comput. Phys. **25**, 205 (1977).
3. G. A. Bird, *Molecular Gas Dynamics and Direct Simulation of Gas Flows* (Clarendon Press, Oxford, 1994).
4. M. E. Jones, D. S. Lemons, R. J. Mason, V. A. Thomas, and D. Winske, J. Comput. Phys. **123**, 169 (1996).
5. W. M. Manheimer, M. Lampe, and G. Joyce, J. Comput. Phys. **138**, 520 (1997, in press)..
6. N. A. Krall and A. W. Trivelpiece, *Principles of Plasma Physics* (McGraw-Hill, New York, 1973), Chap. 6.
7. In order to resolve this very early time, we used smaller time steps $\Delta t = 10^{-9}$ sec in this run. The scattering formulation could be (and otherwise is) run with time steps about an order of magnitude larger.

Martin Lampe, NRL, Code 6709, Washington, DC 20375-5346, (202)767-4041, lampe@ppd.nrl.navy.mil